Available online at www.sciencedirect.com
ScienceDirect
Journal of Power Sources 171 (2007) 861–869
JOURNAL OF POWER SOURCES
www.elsevier.com/locate/jpowsour

Solvent-free, $PYR_{1A}TFSI$ ionic liquid-based ternary polymer electrolyte systems I. Electrochemical characterization

Guk-Tae Kim, Giovanni B. Appetecchi *, Fabrizio Alessandrini, Stefano Passerini **

Ente Per le Nuove Tecnologie, l'Energia e l'Ambiente (ENEA), TER Centro Ricerche Casaccia, Via Anguillarese 301, Rome 00123, Italy

Received 13 April 2007; received in revised form 25 June 2007; accepted 8 July 2007
Available online 17 July 2007

Dedicated to Professor Bruno Scrosati on his 70th birthday anniversary.

Abstract

The electrical properties of solvent-free, PEO–LiTFSI solid polymer electrolytes (SPEs), incorporating different *N*-alkyl-*N*-methylpyrrolidinium bis(trifluoromethanesulfonyl)imide, $PYR_{1A}TFSI$, ionic liquids (ILs), are reported. For this purpose, $PYR_{1A}TFSI$ materials containing side alkyl groups with different chain-length and branching, i.e., *n*-propyl, *sec*-propyl, *n*-butyl, *iso*-butyl, *sec*-butyl and *n*-pentyl, were properly synthesized and homogeneously incorporated into the SPE samples without phase separation. The addition of ILs to PEO–LiTFSI electrolytes results in a large increase of the conductivity and in a decrease of the interfacial resistance with the lithium metal anode. Most of the PEO–LiTFSI–$PYR_{1A}TFSI$ samples showed similar ionic conductivities ($>10^{-4}$ S cm^{-1} at 20 °C) and stable interfacial resistance values (400 Ω cm^2 at 40 °C and 3000 Ω cm^2 at 20 °C) upon several months of storage. Preliminary battery tests have shown that Li/$P(EO)_{10}$LiTFSI + 0.96 $PYR_{1A}TFSI$/$LiFePO_4$ solid-state cells are capable to deliver a capacity of 125 mAh g^{-1} and 100 mAh g^{-1} at 30 °C and 25 °C, respectively.

Keywords: *N*-Alkyl-*N*-methylpyrrolidinium bis(trifluoromethanesulfonyl)imide; Ionic liquid; PEO; Polymer electrolyte

1. Introduction

Lithium metal polymer batteries (LMPBs) are considered excellent candidates for the next generation power sources because of their high-energy density and flexible characteristics [1]. Nevertheless, the performance of LMPBs is still limited by the ionic conductivity of the solvent-free, PEO-based electrolyte. Conductivity values suitable for practical applications ($>10^{-4}$ S cm^{-1}) are approached only at temperatures higher than 70 °C, i.e., above the PEO melting point, because high conductivities in solvent-free polymer electrolytes occur only when the polymer is in the amorphous state [2]. This issue was for more than two decades of years the main drawback for room temperature electrochemical devices. Therefore, several researches were devoted to enhance the conductivity of lithium conducting PEO electrolyte systems.

In this scenario, the incorporation of materials called room-temperature ionic liquid (RTILs) into polymer electrolytes represents a very promising approach. RTILs are molten salts at room temperature that generally consist of an organic cation and an inorganic anion. The main advantages of RTILs towards organic solvents are: non-flammability, negligible vapor pressure, high chemical and thermal stability and, in some cases, hydrophobicity. Therefore, RTILs have attracted a large attention for use as "green" solvents for chemical reactions, bi-phasic catalysis, chemical synthesis, separations, etc. [3–7]. Also, they are under investigation for applications in advanced high-temperature lubricants and heat-transfer fluids in solar thermal energy systems. More recently, RTILs have also been largely investigated as electrolytes (or electrolyte components) for electrochemical applications such as electrodeposition of electropositive metals, photoelectrochemical cells, double-layer

* Corresponding author.
** Corresponding author. Tel.: +39 06 3048 4985; fax: +39 06 3048 6357.
E-mail addresses: gianni.appetecchi@casaccia.enea.it (G.B. Appetecchi), passerini@casaccia.enea.it (S. Passerini).

0378-7753/$ – see front matter © 2007 Elsevier B.V. All rights reserved.
doi:10.1016/j.jpowsour.2007.07.020

capacitors, hybrid super capacitors, fuel cells, and rechargeable lithium batteries [8–23] because of their high ionic conductivity and electrochemical stability.

Particularly, RTILs formed by *N*-alkyl-*N*-methylpyrrolidinium cations $(PYR_{1A})^+$ (the subscripts indicates the number of carbons in the alkyl side chains) and bis(trifluoromethanesulfonyl)imide $(TFSI)^-$ anions have been proposed as electrolyte components for lithium batteries because of their ambient or sub-ambient melting point, high room temperature conductivity and suitable electrochemical stability [24–26]. With respect to unsaturated cyclic and non-cyclic ammonium quaternary cations, pyrrolidinium cations show a much wider cathodic decomposition potential. As an example, $PYR_{14}TFSI$ shows a cathodic stability that exceeds of 1 V that of 1-methyl-3-ethylimidazolium TFSI [27]. Also, imidazolium-based ILs have an unfavorable compatibility towards the lithium metal anode due to the presence of acidic protons and double bounds in the cation [28].

It is well known from literature that the properties of RTILs are related to the nature of their ions. In a previous work [26], we have investigated the influence of the C_AH_{2A+1} alkyl side chain on the electrochemical performance of *N*-alkyl-*N*-methylpyrrolidinium bis(trifluoromethanesulfonyl)imide ($PYR_{1A}TFSI$) ionic liquids. Also, we have successfully demonstrated [17,19–23] that the addition of $PYR_{1A}TFSI$ enhances the ionic conductivity of PEO-based electrolytes (SPEs) above $10^{-4}\,S\,cm^{-1}$ at room temperature without any decrease of the electrochemical stability window of the polymer electrolyte. PEO–LiX–RTIL electrolyte systems were tested at low-medium temperatures in dry, all-solid-state, Li/V_2O_5 and $Li/LiFePO_4$ polymer batteries that delivered large capacity with high reversibility and very good cycling performance at 60 °C. In this paper, we report the effect of the incorporation of several $PYR_{1A}TFSI$ ionic liquids into PEO-based electrolyte systems. The PEO–LiTFSI–$PYR_{1A}TFSI$ polymer electrolyte systems were characterized in terms of ionic conductivity and compatibility towards lithium metal anode. Preliminary room temperature tests were also performed on solid-state $Li/P(EO)_{10}LiTFSI + 0.96\,PYR_{1A}TFSI/LiFePO_4$ batteries.

2. Experimental

2.1. Synthesis of ionic liquids

The $PYR_{1A}TFSI$ ionic liquids were synthesized through a procedure developed at ENEA and described in detail in previous papers [26,29]. The chemicals used, *N*-methylpyrrolidine (97 wt.%), 1-iodopropane (99 wt.%), 2-iodopropane (99 wt.%), 1-iodobutane (99 wt.%), 1-iodo-2-methylpropane (97 wt.%), 2-iodobutane (99 wt.%), 1-iodopentane (98 wt.%), ethyl acetate (ACS grade, >99.5 wt.%), activated carbon (Darco-G60) and alumina (acidic, Brockmann I), were purchased by Aldrich and used as received. LiTFSI salt (99.9 wt.%) was purchased by 3M and used as received. Table 1 summarizes the $PYR_{1A}TFSI$ ionic liquids used for the synthesis of the SPE samples. The chemical structure of the $PYR_{1A}TFSI$ materials is depicted in Fig. 1.

Table 1
$PYR_{1A}TFSI$ ionic liquids incorporated into the PEO-based electrolyte samples

Ionic liquid sample	Acronym
N-Propyl-*N*-methylpyrrolidinium bis(trifluoromethansulfonyl)imide	$PYR_{1n3}TFSI$
sec-Propyl-*N*-methylpyrrolidinium bis(trifluoromethansulfonyl)imide	$PYR_{1sec3}TFSI$
N-Butyl-*N*-methylpyrrolidinium bis(trifluoromethansulfonyl)imide	$PYR_{1n4}TFSI$
iso-Butyl-*N*-methylpyrrolidinium bis(trifluoromethansulfonyl)imide	$PYR_{1iso4}TFSI$
sec-Butyl-*N*-methylpyrrolidinium bis(trifluoromethansulfonyl)imide	$PYR_{1sec4}TFSI$
N-Pentyl-*N*-methylpyrrolidinium bis(trifluoromethansulfonyl)imide	$PYR_{1n5}TFSI$

The water content in the ionic liquids and the polymer electrolyte samples was measured using the standard Karl Fisher method. The titrations were performed by an automatic Karl Fisher titrator (Titralab 90, Radiometer, Copenhagen, Denmark) in dry-room (RH < 0.1%) at 20 °C. The Karl Fisher titrant was a two-component (Hydranal 34800 and Hydranal 34811) reagent provided by Aldrich with a water equivalent of $2.00 \pm 0.02\,mg\,mL^{-1}$ at 20 °C.

2.2. Preparation of polymer electrolytes and composite cathodes

A solvent-free, hot-pressing process developed at ENEA [17,20,21] was used to prepare the PEO–LiTFSI–$PYR_{1A}TFSI$ polymer electrolytes and the composite cathodes. The process was performed in a very low relative humidity dry room (RH < 0.1% at 20 °C). For the electrolyte samples, LiTFSI (3M) and the $PYR_{1A}TFSI$ ionic liquid were dried under vacuum at 110 °C for at least 24 h before use while polyethylene oxide,

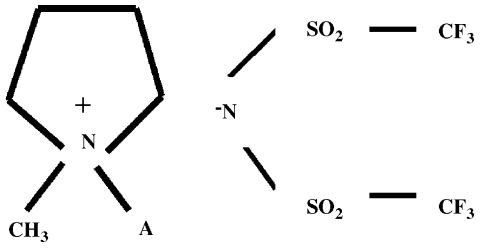

A = *n*-propyl, $-CH_2CH_2CH_3$
A = *iso*-propyl, $-CH(CH_3)_2$
A = *n*-butyl, $-CH_2(CH_2)_2CH_3$
A = *iso*-butyl, $-CH_2CH(CH_3)_2$
A = *sec*-butyl, $-CH(CH_3)(CH_2CH_3)$
A = *n*-pentyl, $-CH_2(CH_2)_3CH_3$

Fig. 1. Chemical structure of the $PYR_{1A}TFSI$ ionic liquids incorporated into the PEO electrolyte samples.

Table 2
Mole composition and electrical conductivity of the PEO–LiTFSI–$PYR_{1A}TFSI$ polymer electrolyte samples at 20 °C and 60 °C

Polymer electrolyte composition [0.96 = $(PYR_{1A})^+/Li^+$ mole ratio]	Sample acronym	Conductivity (S cm^{-1})	
		20 °C	60 °C
$P(EO)_{10}LiTFSI$	IL-free	$(1.33 \pm 0.09) \times 10^{-6}$	$(3.5 \pm 0.1) \times 10^{-4}$
$P(EO)_{10}LiTFSI + 0.96\ PYR_{1n3}TFSI$	PEO–PYR_{1n3}	$(1.38 \pm 0.06) \times 10^{-4}$	$(1.2 \pm 0.1) \times 10^{-3}$
$P(EO)_{10}LiTFSI + 0.96\ PYR_{1sec3}TFSI$	PEO–PYR_{1sec3}	$(2.02 \pm 0.09) \times 10^{-6}$	$(7.6 \pm 0.6) \times 10^{-4}$
$P(EO)_{10}LiTFSI + 0.96\ PYR_{1n4}TFSI$	PEO–PYR_{1n4}	$(1.11 \pm 0.05) \times 10^{-4}$	$(1.0 \pm 0.1) \times 10^{-3}$
$P(EO)_{10}LiTFSI + 0.96\ PYR_{1iso4}TFSI$	PEO–PYR_{1iso4}	$(1.28 \pm 0.06) \times 10^{-4}$	$(1.2 \pm 0.1) \times 10^{-3}$
$P(EO)_{10}LiTFSI + 0.96\ PYR_{1sec4}TFSI$	PEO–PYR_{1sec4}	$(1.05 \pm 0.05) \times 10^{-4}$	$(1.1 \pm 0.1) \times 10^{-3}$
$P(EO)_{10}LiTFSI + 0.96\ PYR_{1n5}TFSI$	PEO–PYR_{1n5}	$(1.03 \pm 0.05) \times 10^{-4}$	$(1.0 \pm 0.1) \times 10^{-3}$

PEO (Union Carbide, WSR 301, M_W = 4,000,000), was dried at 50 °C for 48 h. PEO and LiTFSI (EO/Li mole ratio = 10) was intimately mixed in a mortar and then $PYR_{1A}TFSI$ was added to achieve a $(PYR_{1A})^+/Li^+$ mole ratio equal to 0.96 [23]. The PEO–LiTFSI–$PYR_{1A}TFSI$ mixtures were annealed under vacuum at 100 °C overnight. Finally, the homogeneous, plastic-like materials obtained were hot-pressed at 100 °C for 2 min to obtain 70–80 μm thick films. The mole composition of the PEO–LiTFSI–$PYR_{1A}TFSI$ polymer electrolytes is reported in Table 2.

The composite cathode was prepared by intimately mixing $LiFePO_4$ (active material synthesized at ENEA [30], 43 wt.%) and carbon (KJB, Akzo Nobel, 7 wt.%), which were previously dried in a vacuum oven at 120 °C for at least 24 h. PEO (17.5 wt.%), LiTFSI (5 wt.%) and $PYR_{1n4}TFSI$ (27.5 wt.%) were mixed to obtain a paste-like mixture that was added to the previous blend. The final mixture was firstly annealed at 100 °C overnight and then hot-pressed to form thick stripes (about 1 mm thick) of composite cathode. The stripes were cold-calendered to form the 0.05 mm thick cathode films.

The water content of the electrolyte and composite cathode films was lower than 20 ppm as confirmed by Kark–Fisher titration.

2.3. Test cells assembly

The conductivity and interfacial stability measurements on the $P(EO)_{10}LiTFSI + 0.96\ PYR_{1A}TFSI$ polymer electrolyte samples were performed on sealed, laminated, two-electrode cells fabricated inside the dry-room. The tests cells were assembled by sandwiching a polymer electrolyte film between two copper (conductivity measurements) or lithium (Li/polymer electrolyte interfacial stability measurements) foils. The assembled cells were housed in sealed, laminated aluminum (coffee-bag like) envelopes and successively laminated twice by hot-rolling at 100 °C. The electrochemical active area of the laminated cells approached 10 cm^2.

The solid-state $Li/LiFePO_4$ batteries (cathode limited) were fabricated by laminating a lithium foil (50 μm thick), a $P(EO)_{10}LiTFSI + 0.96\ PYR_{1n4}TFSI$ polymer electrolyte membrane and a $LiFePO_4$-based cathode film. The assembled cells were housed in sealed, coffee-bag envelopes and successively laminated twice by hot-rolling at 100 °C. The electrochemical active area of the laminated cells approached 1 cm^2.

2.4. Electrochemical tests

The ionic conductivity of the polymer electrolytes and their interfacial stability with lithium anode were determined by impedance measurements taken on Cu/SPE/Cu or Li/SPE/Li cells, respectively. The AC tests were performed by means of a Frequency Response Analyzer (F.R.A., Schlumberger Solartron 1260) in the 1 Hz–100 kHz (conductivity tests) and 10 mHz–65 kHz (interfacial stability tests) frequency ranges, respectively.

The conductivity tests were performed on a heating stepped ramp from −40 °C to 100 °C. Prior to perform the temperature ramp the Cu/SPE/Cu cells were held at −40 °C for 24 h to avoid slow kinetic effects on the polymer electrolytes. The temperature was changed in 10 °C steps every 24 h to allow a complete thermal equilibration of the cells before each measurement. The interfacial stability measurements were taken in a temperature range from 20 °C to 40 °C. For both experiments the cells were located in a cold/heat test chamber Binder GmbH MK53 with a temperature control of ±0.1 °C.

The impedance responses were analyzed using the well-known Non-Linear Least-Square (NLLSQ) fit software [31–33]. Both the conductivity tests and the interfacial resistance measurements were carried out on at least three different cells for each polymer electrolyte in order to verify the reproducibility of the obtained results.

The cycling tests on full $Li/LiFePO_4$ batteries were performed at temperatures ranging from 20 °C to 40 °C range at *C*/10 rate (corresponding to 0.1 mA cm^{-2}) using a MACCOR S4000 battery tester. The voltage cut-offs were fixed at 4.0 V (charge step) and 2.0 V (discharge step), respectively.

3. Results and discussion

The $PYR_{1A}TFSI$ compounds used to form the ternary PEO–LiTFSI–$PYR_{1A}TFSI$ polymer electrolyte systems exhibit a melting point ranging from about −5 °C to +10 °C [26], i.e., below the room temperature. Therefore, they may be claimed as room temperature ionic liquids (RTILs) with the exception of $PYR_{1sec3}TFSI$. This latter compound melts above 100 °C and cannot be considered as an ionic liquid [34], however, it was used for comparison reasons.

The $P(EO)_{10}LiTFSI + 0.96\ PYR_{1A}TFSI$ films appeared very homogeneous even after prolonged storage times, e.g., more than

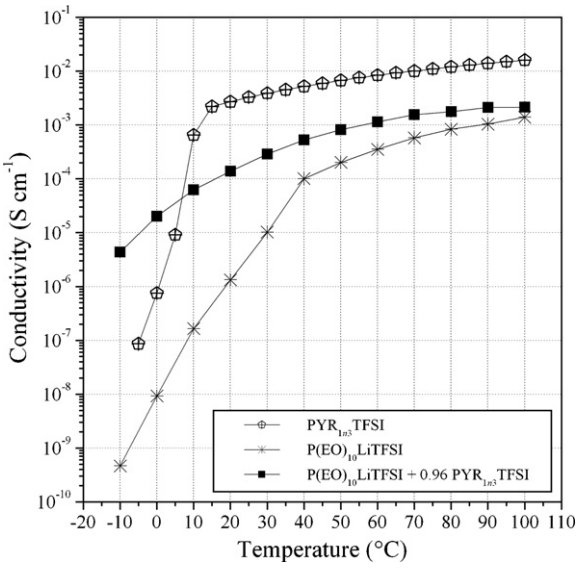

Fig. 2. Conductivity vs. temperature behavior of neat $PYR_{1n3}TFSI$ ionic liquid, $P(EO)_{10}LiTFSI$ and $P(EO)_{10}LiTFSI + 0.96\,PYR_{1n3}TFSI$ polymer electrolytes.

1 year. No phase separation and/or syneresis phenomenon, i.e., ionic liquid release, was observed for the samples thus suggesting a high physico-chemical stability of the ternary electrolyte systems. On the other hand, the binary mixtures of PEO and the $PYR_{1A}TFSI$ ionic liquids were found to be unstable. These binary mixtures showed a marked phase separation (indicated by the presence of ionic liquid on the surfaces of the polymer electrolyte films) within 2–3 weeks. For such a reason the binary mixtures were not further investigated.

3.1. Ionic transport properties of PEO–LiX–$PYR_{1A}TFSI$

The ionic conductivity (σ) of the $P(EO)_{10}LiTFSI + 0.96\,PYR_{1A}TFSI$ polymer electrolyte samples was determined from the impedance measurements by using the following equation:

$$\sigma = \frac{t}{A}\frac{1}{R} \tag{1}$$

where t, A and R represent, respectively, the thickness, the active area and the ionic resistance of the sample. The experimental error, $\Delta\sigma$, on the conductivity was evaluated using the following equation:

$$\Delta\sigma = \left|\frac{\partial\sigma}{\partial t}\right|\Delta t + \left|\frac{\partial\sigma}{\partial A}\right|\Delta A + \left|\frac{\partial\sigma}{\partial R}\right|\Delta R \tag{2}$$

where Δt, ΔA and ΔR represent the errors associated with the thickness, the active area and the ionic resistance of the sample, respectively. ΔR takes into account both the error due to the AC impedance equipment and the analysis fitting program.

Fig. 2 compares the conductivity versus temperature dependence of the neat $PYR_{1n3}TFSI$ ionic liquid (data taken from Ref. [26]), $P(EO)_{10}LiTFSI$ (IL-free) and $P(EO)_{10}LiTFSI + 0.96\,PYR_{1n3}TFSI$ polymer electrolytes. As expected, the IL-free sample exhibits two different trends of the conductivity versus temperature behavior with a slope change at around 40 °C. This behavior is very typical of PEO–LiX electrolytes with the slope change coinciding to the melting of the salt reach phase [2]. Analogously, the neat $PYR_{1n3}TFSI$ shows two linear trends with a knee at about 15 °C due to the melting of the material [26]. On the other hand, the $P(EO)_{10}LiTFSI + 0.96\,PYR_{1n3}TFSI$ electrolyte exhibits a VTF-like behavior [35] typical of completely amorphous ionic conductors [36–38]. This behavior is maintained even in the temperature range in which the neat RTIL and PEO–LiTFSI are crystalline. The comparison of the three curves in Fig. 2 clearly shows the beneficial effect of the addition of the RTILs on the conductivity of PEO-based electrolytes. At room temperature (20 °C) the ternary polymer electrolyte shows a conductivity value larger than $10^{-4}\,S\,cm^{-1}$ (see Table 2), which is two orders of magnitude higher than that of the RTIL-free sample. At 60 °C, the $P(EO)_{10}LiTFSI + 0.96\,PYR_{1n3}TFSI$ electrolyte still exhibits a substantially higher conductivity (ca. $10^{-3}\,S\,cm^{-1}$) than the RTIL-free electrolytes. At sub-ambient temperatures the increase in conductivity is even more marked (four orders of magnitude at −10 °C). The low temperature conductivity increase is ascribable to the interaction between the RTIL and LiTFSI [39,40] that prevents the formation of the crystalline $P(EO)_6LiTFSI$ phase [20]. Also interesting to point out is that the low temperature conductivity of the ternary system is higher than that of the neat ionic liquid and its mixtures with LiTFSI [40]. The complex interactions that hinder the crystallization of the single components and the binary mixtures (PEO–LiTFSI and IL–LiTFSI) in the ternary system are not known yet. However, Raman [39] and NMR [40] measurements have indicated that in LiTFSI–$PYR_{1n3}TFSI$ mixtures all the $TFSI^-$ anions interact strongly with the Li^+ cations. In the $0.33LiTFSI–0.66PYR_{1n3}TFSI$ crystalline compound all three $TFSI^-$ anions (one from the lithium salt and two from the RTIL) have been seen involved in the coordination of the densely charged Li^+ cations [39]. We can suppose that this $Li^+\cdots TFSI^-$ interaction plays a role in the ternary system PEO–LiTFSI–$PYR_{1A}TFSI$ reducing the role of the PEO chains in the coordination of the Li^+ cations, which would prevent the formation of the $P(EO)_6LiTFSI$ crystalline complex. NMR and Raman studies of the ternary systems are presently on-going in our laboratories to verify this hypothesis. Nevertheless, the ternary system maintains an appreciable conductivity at temperatures lower than the melting point of the single components.

The temperature dependence of the ionic conductivity of the $P(EO)_{10}LiTFSI + 0.96\,PYR_{1A}TFSI$ electrolytes as a function of the $(PYR_{1A})^+$ cation side chain (A) is depicted in the Arrhenius plot reported in Fig. 3 (see legend for details). The conductivity of the IL-free binary electrolyte is reported for comparison purpose. The error bars, when not reported, fall within the data point markers.

With the exception of the polymer electrolyte containing $PYR_{1sec3}TFSI$ all the ternary polymer electrolytes showed the VTF-like behavior previously seen for $P(EO)_{10}TFSI + 0.96\,PYR_{1n3}TFSI$ (Fig. 2). This evidence indicates that these ternary electrolytes are amorphous in the temperature range investigated. In addition, the ternary electrolytes have very similar conductivities, e.g., $10^{-4}\,S\,cm^{-1}$ at 20 °C and $10^{-3}\,S\,cm^{-1}$ at 60 °C (Table 2). The slightly higher conductivity observed

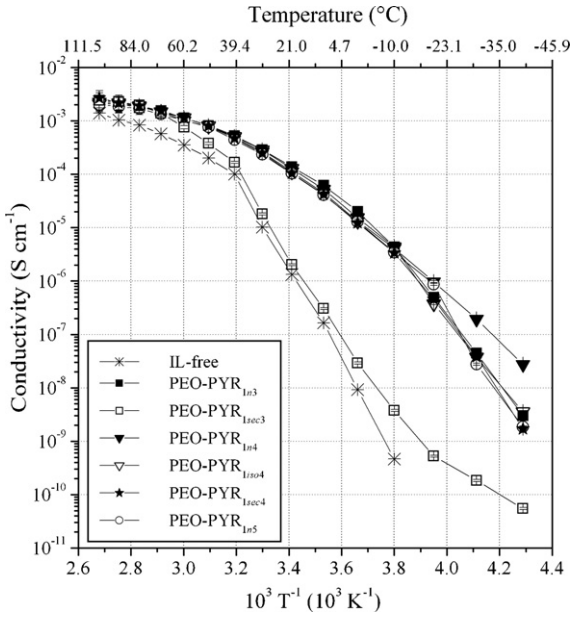

Fig. 3. Arrhenius conductivity plot of various $P(EO)_{10}LiTFSI + 0.96\,PYR_{1A}TFSI$ polymer electrolytes (see legend). The data referred to the $PYR_{1A}TFSI$-free sample are reported for comparison purpose.

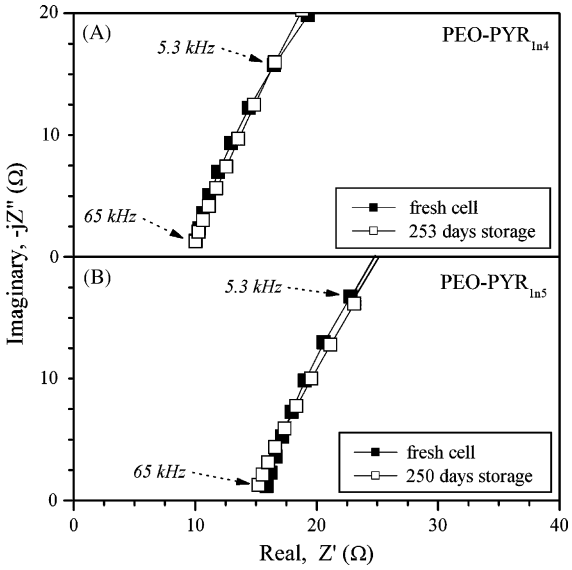

Fig. 4. High frequencies range of the impedance response of Li/PEO–PYR_{1n4}/Li (A) and Li/PEO–PYR_{1n5}/Li (B) cells taken at different storage times (see legend). $T = 20\,^{\circ}C$.

below $-20\,^{\circ}C$ for the $PYR_{1n4}TFSI$-containing electrolyte is most likely correlated with the substantially lower melting point of this RTIL ($T_m = -5\,^{\circ}C$) [26] with respect to the other RTILs (T_m between $10\,^{\circ}C$ and $12\,^{\circ}C$) [26]. To summarize, the change of the side chain length or the branching of the pyrrolidinium cation side chain does not introduce any substantial differences in the conductivity versus temperature behavior of the ternary electrolytes with the exception of $P(EO)_{10}LiTFSI + 0.96\,PYR_{1sec3}TFSI$ that exhibits a VTF-like behavior only above $40\,^{\circ}C$, i.e., like the binary PEO–LiTFSI electrolyte.

3.2. Chemical stability and interfacial properties

The chemical stability and the interfacial properties of the $P(EO)_{10}LiTFSI + 0.96\,PYR_{1A}TFSI$ polymer electrolytes at the interface with the lithium metal anode were evaluated by following the time evolution of the impedance response of Li/polymer electrolyte/Li cells stored at different temperatures.

Fig. 4 magnifies the AC responses of the Li/PEO–PYR_{1n4}/Li and Li/PEO–PYR_{1n5}/Li cells in the high frequency region. The intercept of the AC response with the real axis corresponds to the electrolyte resistance [31]. The measurements were taken at $20\,^{\circ}C$ on the cells as made and after 250 days of storage during which the cells were subjected to repeated heating/cooling steps. As it is clearly seen in the figure, no feature change of the AC plot of the RTIL-containing polymer electrolytes was observed even after such a prolonged storage time. The stability of the impedance response indicates that phase separation did not take place in the electrolytes (because it would result in a change of their bulk ionic resistances).

Fig. 5 reports the Nyquist plot of Li/$P(EO)_{10}LiTFSI + 0.96\,PYR_{1A}TFSI$/Li cells kept at temperatures ranging from $20\,^{\circ}C$ to $40\,^{\circ}C$. The AC responses referring to the IL-free sample are also depicted for comparison purpose. The impedance responses were normalized towards the electrochemically active area of the cells. All $P(EO)_{10}LiTFSI + 0.96\,PYR_{1A}TFSI$ electrolytes showed a slightly depressed semicircle, associated with the lithium–polymer electrolyte interfacial processes [31]. The diameter of the semicircle is related to the overall interfacial resistance (R_i) that takes into account the charge transfer resistance at the Li/polymer electrolyte interface (R_{CT}) as well as the additional impedance (R_P) associated with the growth of a passive layer at such an interface, e.g., $R_i = R_{CT} + R_P$. The AC plots of Fig. 5 indicate that the shape of the impedance responses, typical of Li/polymer electrolyte/Li cells, does not substantially change with the temperature and/or the nature of the $PYR_{1A}TFSI$ ionic liquid. However, a substantial reduction of the semicircles, that corresponds to a decrease of the interfacial resistance of about one order of magnitude, is observed on increasing the cell temperature from $20\,^{\circ}C$ to $40\,^{\circ}C$. It is also interesting to point out that the interfacial resistance of the IL-free sample is higher than that of the $PYR_{1A}TFSI$-containing polymer electrolytes.

The normalized interfacial resistance, R_N, of the $P(EO)_{10}LiTFSI + 0.96\,PYR_{1A}TFSI$ polymer electrolyte samples in contact with a lithium anode was determined by using the following equation:

$$R_N = \frac{R_i}{2} A \tag{3}$$

where R_i and A represent, respectively, the interface resistance and the electrochemically active electrode area of the Li/SPE/Li test cells. The interface resistance values for the different test cells were obtained from the fitting analysis of the impedance responses. The experimental errors, ΔR_N, on the interface resis-

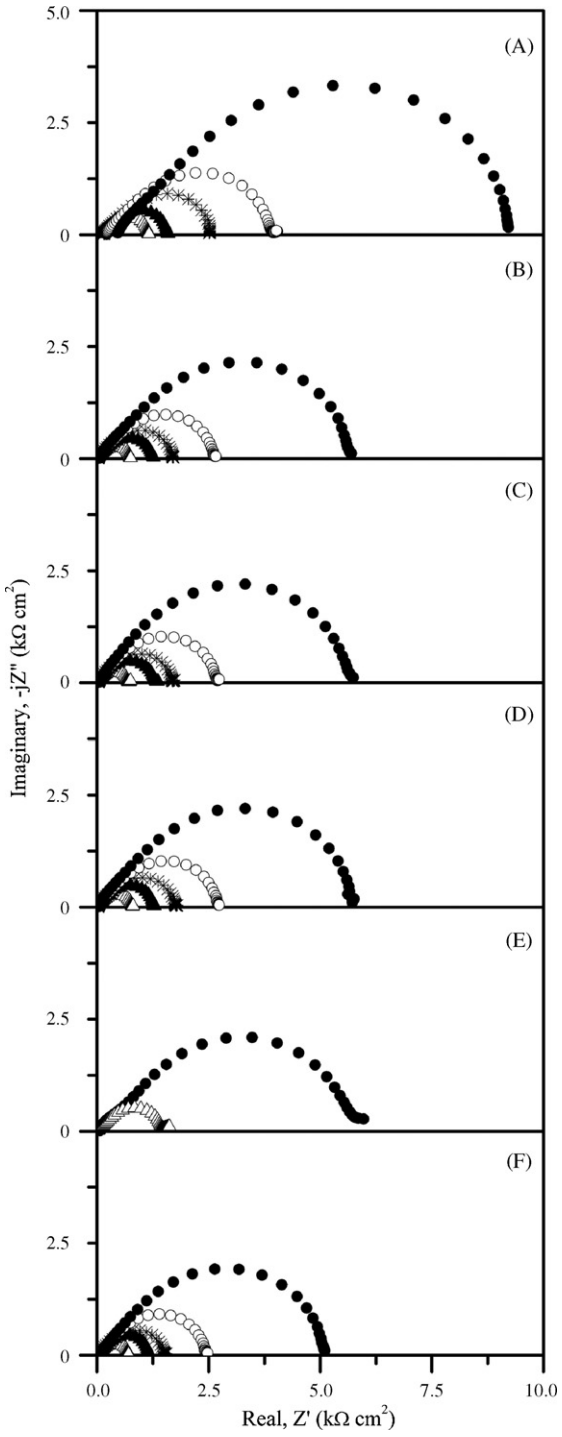

Fig. 5. AC responses of Li/P(EO)$_{10}$LiTFSI + 0.96 PYR$_{1A}$TFSI/Li cells stored at different temperatures (open triangle: 40 °C; solid triangle: 35 °C; star: 30 °C; open circle: 25 °C; solid circle: 20 °C). Panels from A to F are referred to IL-free (A), PEO–PYR$_{1n3}$ (B), PEO–PYR$_{1n4}$ (C), PEO–PYR$_{1iso4}$ (D), PEO–PYR$_{1sec4}$ (E) and PEO–PYR$_{1n5}$ (F) samples, respectively.

tance was evaluated using the following equation:

$$\Delta R_N = \left|\frac{\partial R_N}{\partial R_i}\right| \Delta R_i + \left|\frac{\partial R_N}{\partial A}\right| \Delta A \quad (4)$$

where ΔR_i and ΔA represent the errors associated with the interface resistance and the active area of the test cell sample, respectively. ΔR_i takes into account the error due to both the AC impedance equipment and the fitting program.

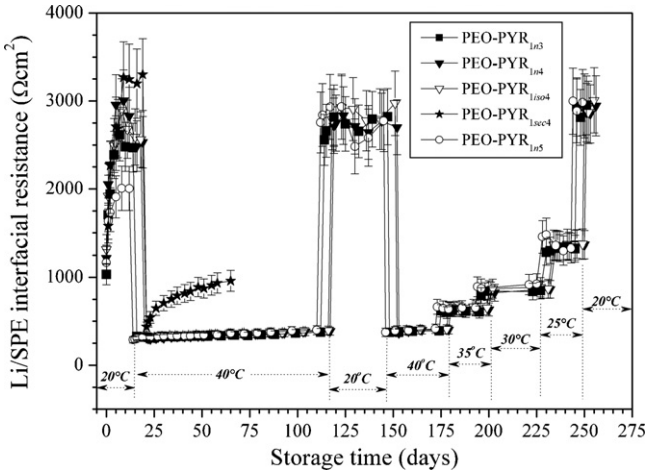

Fig. 6. Time evolution of the interfacial resistance of various P(EO)$_{10}$LiTFSI + 0.96 PYR$_{1A}$TFSI polymer electrolytes (see legend) in contact with a lithium metal anode at different temperatures. The interface resistance values were normalized towards the active area of the test cells.

The evolution of the interface resistance versus storage time and temperature of various P(EO)$_{10}$LiTFSI + 0.96 PYR$_{1A}$TFSI polymer electrolytes in symmetric lithium cells is shown in Fig. 6. The storage tests were performed for more than 8 months during which the cells were monitored by measuring their impedance daily. The storage temperature was changed to investigate its effect on the lithium/polymer electrolyte interfaces. Initially, the cells were stored at 20 °C for 15 days. After this period, the storage temperature was increased to 40 °C for 100 days and, then, again reduced to 20 °C for additional 30 days. Successively, the cells were kept at 40 °C for 35 days and, finally, the temperature was decreased from 40 °C to 20 °C in 5 °C steps every 20–25 days.

During the initial period of storage at 20 °C, a marked increase of R_N was observed for all cells while in the following part of the test (8 months) the interfacial resistance was found to be constant with the exception of the polymer electrolyte containing PYR$_{1sec4}$TFSI. The anomalous behavior of this polymer electrolyte is most likely associated with the lower electrochemical stability of PYR$_{1sec4}$TFSI [26] that result in the higher reactivity of the polymer electrolyte towards the lithium metal. As a result of the poor stability of the interface with lithium the tests on the polymer electrolyte containing PYR$_{1sec4}$TFSI were discontinued.

The initial increase of R_N and its following substantial stability (even after long storage periods) is commonly observed in dry, solvent-free PEO electrolytes [41–43]. The initial increase is due to the reaction between the lithium metal electrode and the polymer electrolyte to form a passive layer (called SEI) [31] onto the lithium anode that protects the electrode from further reaction. The kinetics of the passive layer formation appears to depend on the nature of the PYR$_{1A}$TFSI used. However, the differences observed at the end of the first storage period (see Fig. 6) disappeared almost completely on increasing the storage temperature. As a matter of fact, all cells showed

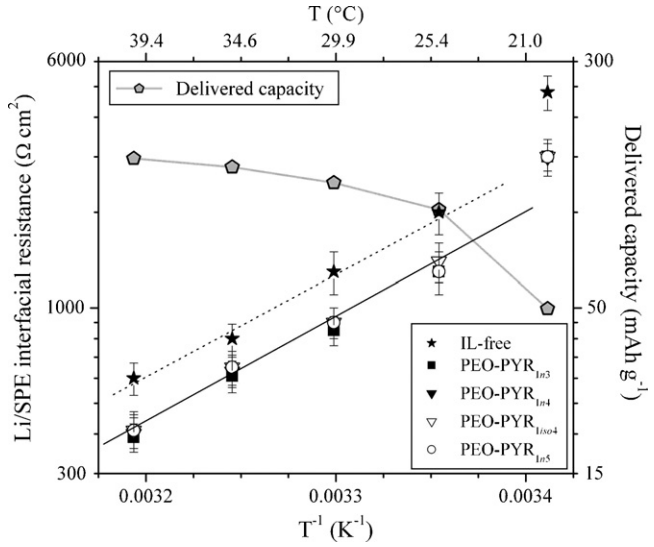

Fig. 7. Interfacial resistance vs. temperature dependence of selected $P(EO)_{10}LiTFSI + 0.96\,PYR_{1A}TFSI$ polymer electrolyte samples (see legend). The data referred to the IL-free sample are reported for comparison purpose. The interface resistance values were normalized towards the active area of the test cells. The discharge capacity vs. temperature behavior, referred to a $Li/P(EO)_{10}LiTFSI + 0.96\,PYR_{1n4}TFSI/LiFePO_4$ full battery, is also reported.

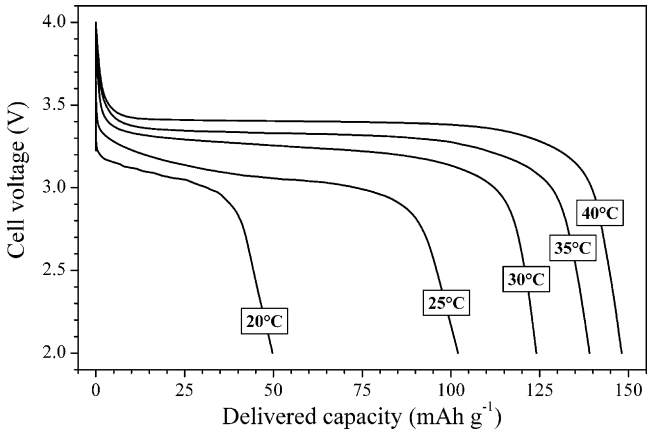

Fig. 8. Voltage vs. delivered capacity profile referred to selected discharge steps, obtained at different temperatures, of a $Li/P(EO)_{10}LiTFSI + 0.96\,PYR_{1n4}TFSI/LiFePO_4$ full battery. Rate: $C/10$. Current density: 0.1 mA cm^{-2}.

very near interfacial resistance values (within the experimental error) during the prolonged storage at 40 °C. Nevertheless, a slight increase of the interfacial resistance is also observed in this period. However, after the second storage period at 20 °C, the RTIL-containing electrolytes exhibited time-stable interfacial resistance values of about 400 Ω cm^2 and 3000 Ω cm^2 at 40 °C and 20 °C, respectively. This evidence supports for a substantial long-term stability of the interface formed between the lithium metal electrode and the ternary polymer electrolytes containing the $PYR_{1n3}TFSI$, $PYR_{1n4}TFSI$, $PYR_{1iso4}TFSI$, and $PYR_{1n5}TFSI$ RTILs. The dependence of the interfacial resistance as a function of the inverse of the temperature for these polymer electrolytes (see Fig. 7 and Table 3) is seen to be linear between 25 °C and 40 °C. The slope of this curve is related to the activation energy (E_a) of the charge transfer process by the following equation [44,45]:

$$R_N = A\, e^{E_a/kT} \quad (5)$$

where A is a parameter that depends on the charge carrier number and k is the Boltzmann constant. The charge transfer E_a values obtained for the RTIL-containing polymer electrolytes are reported in Table 3 together with the one of the RTIL-free polymer electrolyte. All materials including the IL-free electrolyte exhibit very similar activation energies (around 60 kJ mol^{-1}) that supports for a strong similarity of the charge transfer process (at least in the 25–40 °C temperature range). Therefore, the lower interface resistance of the RTIL-containing polymer electrolytes should be ascribed to the lower thickness of the SEI layer formed at the Li/SPE interface.

The substantial discontinuity of the interfacial resistance observed at 20 °C, i.e., the values at this temperature are seen to stand far above the trend line drawn from the R_N values at higher temperatures, is indicative of a substantial activation energy increase for the charge transfer process most likely due to a reduced mobility of the Li^+ cations into the SEI at this temperature. Nevertheless, the ternary electrolytes always showed lower interfacial impedance values than the RTIL-free electrolyte.

To summarize, the investigation of the Li/polymer electrolyte interface reveals that the addition of the RTILs to the PEO–LiTFSI electrolyte improves the performance of the interface with lithium metal, in particular at temperatures lower than 30 °C.

3.3. Battery tests

Preliminary low temperature cycling tests (see Fig. 8) were performed on solid-state $Li/LiFePO_4$ (specific capac-

Table 3
Interfacial resistances of selected $P(EO)_{10}LiTFSI + 0.96\,PYR_{1A}TFSI$ electrolyte samples in contact with a lithium metal anode at different temperatures

Sample	Li/SPE interface resistance (Ω cm^2)					E_a (kJ mol^{-1})
	20 °C	25 °C	30 °C	35 °C	40 °C	
IL-free	4800 ± 600	2000 ± 300	1300 ± 200	800 ± 90	600 ± 70	60 ± 10
$PEO–PYR_{1n3}$	3000 ± 300	1300 ± 200	850 ± 90	610 ± 70	390 ± 40	61 ± 9
$PEO–PYR_{1n4}$	3000 ± 300	1400 ± 200	900 ± 100	630 ± 70	400 ± 50	60 ± 10
$PEO–PYR_{1iso4}$	3000 ± 400	1400 ± 200	900 ± 100	650 ± 80	410 ± 50	60 ± 10
$PEO–PYR_{1n5}$	3000 ± 400	1300 ± 200	900 ± 100	650 ± 80	410 ± 60	60 ± 10

The activation energy values are also reported. For comparison purpose, the data obtained for the IL-free polymer electrolyte are also reported.

ity of 154 mA g^{-1} [30]) battery using $P(EO)_{10}LiTFSI + 0.96$ $PYR_{1n4}TFSI$ as the electrolyte. The maximum delivered capacity (see Fig. 7) was about 150 mAh g^{-1} (97.4% of the nominal capacity) at 40 °C. The battery was able to deliver more than 100 mAh g^{-1} (65%) at 25 °C. However, a large capacity decrease was observed at 20 °C where only about 50 mAh g^{-1} (32%) were delivered. The reason of such a decrease is found comparing the discharge curves at different temperatures (see Fig. 8). At or above 30 °C the discharge curves show a flat discharge plateau in the 3.4–3.2 V range, typical of Li/SPE/$LiFePO_4$ batteries [23]. At lower temperatures (<30 °C) the flat voltage region is seen to progressively shorten and decrease to 3.0 V while the initial ohmic drop (IR) is seen to jump from 390 mV at 30 °C to 720 mV at 20 °C. Simple calculations show that the cell resistance from the IR drop was 3500 Ω at 40 °C, 3900 Ω at 30 °C and 7200 Ω at 20 °C, i.e., much higher than the calculated electrolyte resistances, 16 Ω at 40 °C, 31 Ω at 30 °C and 73 Ω at 20 °C, but very similar to the lithium/SPE interface resistance values reported earlier. As a matter of fact, the dependence of the discharge capacity as a function of the temperature (see Fig. 7) shows the opposite trend with respect to the one exhibited by the interfacial resistance. The capacity decreases almost linearly on decreasing temperatures with a steeper decrease observed below 25 °C. This clearly indicates that the performance decay of the Li/$P(EO)_{10}LiTFSI + 0.96\,PYR_{1n4}TFSI/LiFePO_4$ battery at low temperatures is most likely associated to the strong increase of the SEI resistance below 25 °C.

4. Conclusions

Solvent-free, PEO–LiTFSI solid polymer electrolytes, incorporating *N*-alkyl-*N*-methylpyrrolidinium bis(trifluoromethanesulfonyl)imide, ($PYR_{1A}TFSI$) ionic liquids, were prepared and characterized.

The PEO–LiTFSI–$PYR_{1A}TFSI$ ternary systems show good mechanical properties with a high stability even after prolonged storage. The addition of RTILs to PEO–LiTFSI electrolytes resulted in a large increase of the ionic conductivity and in a decrease of the SEI resistance with the lithium electrode. The PEO–LiTFSI–$PYR_{1A}TFSI$ electrolytes showed ionic conductivities higher than 10^{-4} S cm^{-1} at 20 °C and stable interfacial resistances (400 Ω cm^2 at 40 °C and 3000 Ω cm^2 at 20 °C) upon several months of storage in contact with lithium metal. No practical differences were observed with the length and the branching of the $PYR_{1A}{}^+$ cation side-chain group with the exception of $(PYR_{1sec4})^+$ and $(PYR_{1sec3})^+$.

Preliminary battery tests have shown that Li/$P(EO)_{10}$ $LiTFSI + 0.96\,PYR_{1A}TFSI/LiFePO_4$ solid-state cells are capable of delivering high capacity at near room temperatures (125 mAh g^{-1} and 150 mAh g^{-1} at 30 °C and 40 °C, respectively). The performance decay observed at 20 °C is ascribed to the strong increase of the SEI resistance below 25 °C. However, this work demonstrates that the search for new solvent-free polymer electrolytes for lithium rechargeable batteries has not ended yet.

Acknowledgements

G.-T. Kim acknowledges the Italian Foreign Ministry and the Korea Research Foundation Grant (MOEHRD) (KRF-2005-214-D00295) for the financial support.

References

[1] J.M. Tarascon, M. Armand, Nature (London) 414 (2001) 359.
[2] R. Frech, S. Chintapalli, P.G. Bruce, C.A. Vincent, Macromolecules 32 (1999) 808.
[3] P. Wasserscheid, W. Keim, Angew. Chem. Int. Ed. 39 (2000) 3772.
[4] R.D. Rogers, K.R. Seddon (Eds.), Ionic Liquids—Industrial Application to Green Chemistry, ACS Symposium Series 818, Oxford University Press, 2002.
[5] M.J. Earle, K.R. Seddon, Pure Appl. Chem. 72 (2000) 1391.
[6] J.L. Anderson, J. Ding, T. Welton, D.W. Armstrong, J. Am. Chem. Soc. 124 (2002) 14247.
[7] J. Dupont, R.F. de Souza, P.A.Z. Suarez, Chem. Rev. 102 (2002) 3667.
[8] A.I. Bhatt, I. May, V.A. Volkovich, M.E. Hetherington, B. Lewin, R.C. Thied, N. Ertok, J. Chem. Soc., Dalton Trans. 4532 (2002).
[9] S. Panozzo, M. Armand, O. Stephan, Appl. Phys. Lett. 80 (2002) 679.
[10] P. Wang, S.M. Zakeeruddin, I. Exnar, M. Gratzel, Chem. Commun. 2972 (2002).
[11] J. Fuller, A.C. Breda, R.T. Carlin, J. Electroanal. Chem. 459 (1998) 29.
[12] H. Nakagawa, S. Izuchi, K. Kunawa, T. Nukuda, Y. Aihara, J. Electrochem. Soc. 150 (2003) A695.
[13] H. Sakaebe, H. Matsumoto, Electrochem. Commun. 5 (2003) 594.
[14] A. Noda, M.A.B.H. Susan, K. Kudo, S. Mitsushima, K. Hayamizu, M. Watanabe, J. Phys. Chem. B 107 (2003) 4024.
[15] A. Balducci, W.A. Henderson, M. Mastragostino, S. Passerini, P. Simon, F. Soavi, Electrochim. Acta 50 (2005) 2233.
[16] Y.S. Fuang, R.Q. Zhou, J. Power Sources 81 (1999) 891.
[17] J.-H. Shin, W.A. Henderson, S. Passerini, Electrochem. Commun. 5 (2003) 1016.
[18] A. Lewandowski, A. Swiderska, Solid State Ionics 169 (2004) 21.
[19] J.-H. Shin, W.A. Henderson, S. Passerini, Electrochem. Solid-State Lett. 8 (2005) A125.
[20] J.-H. Shin, W.A. Henderson, S. Passerini, J. Electrochem. Soc. 152 (2005) A978.
[21] J.-H. Shin, W.A. Henderson, G.B. Appetecchi, F. Alessandrini, S. Passerini, Electrochim. Acta 50 (2005) 3859.
[22] J.-H. Shin, W.A. Henderson, S. Scaccia, P.P. Prosini, S. Passerini, J. Power Sources 156 (2006) 560.
[23] J.-H. Shin, W.A. Henderson, C. Tizzani, S. Passerini, S.-S. Jeong, K.-W. Kim, J. Electrochem. Soc. 153 (9) (2006) A1649.
[24] D.R. MacFarlane, J. Sun, M. Forsyth, P. Meakin, N. Amini, J. Phys. Chem. B 103 (1999) 4164.
[25] D.R. MacFarlane, J. Huang, M. Forsyth, Nature (London) 402 (1999) 792.
[26] G.B. Appetecchi, D. Zane, F. Alessandrini, S. Passerini, Electrochim. Acta, submitted for publication.
[27] Z.B. Zhou, H. Matsumoto, K. Tatsumi, Chem. Eur. J. 12 (2006) 2196.
[28] V.R. Koch, C. Nanjundiah, G.B. Appetecchi, B. Scrosati, J. Electrochem. Soc. 142 (1995) L116.
[29] G.B. Appetecchi, S. Scaccia, C. Tizzani, F. Alessandrini, S. Passerini, J. Electrochem. Soc. 153 (9) (2006) A1685.
[30] P.P. Prosini, M. Carewska, S. Scaccia, P. Wisniewski, S. Passerini, M. Pasquali, J. Electrochem. Soc. 149 (2002) A886.
[31] J.R. MacDonald (Ed.), Impedance Spectroscopy, John Wiley & Sons, New York, 1987.
[32] B.A. Boukamp, Solid State Ionics 18 (1986) 136.
[33] B.A. Boukamp, Solid State Ionics 20 (1986) 31.
[34] P. Wasserscheid, T. Welton (Eds.), Ionic Liquids in Synthesis, Wiley-VCH, Weinheim, 2003.

[35] H. Vogel, Phys. Z. 22 (1921) 645;
G.S. Fulcher, J. Am. Chem. Soc. 8 (1925) 339;
G. Tamman, W. Hesse, Z. Anorg. Allg. Chem. 156 (1926) 245.
[36] S. Lascaud, M. Perrier, A. Valle'e, S. Besner, J. Prud'homme, M. Armand, Macromolecules 27 (1994) 7469.
[37] G.B. Appetecchi, G. Dautzenberg, B. Scrosati, J. Electrochem. Soc. 143 (1996) 6.
[38] Y. Aihara, G.B. Appetecchi, B. Scrosati, J. Electrochem. Soc. 149 (2002) A849.
[39] M. Castriota, T. Caruso, R.G. Agostino, E. Cazzanelli, W.A. Henderson, S. Passerini, J. Phys. Chem. A 109 (2005) 92.
[40] I. Nicotera, C. Oliviero, W.A. Henderson, G.B. Appetecchi, S. Passerini, J. Phys. Chem. B 109 (2005) 22814.
[41] G.B. Appetecchi, S. Scaccia, S. Passerini, J. Electrochem. Soc. 147 (2000) 4448.
[42] G.B. Appetecchi, F. Alessandrini, M. Carewska, T. Caruso, P.P. Prosini, S. Scaccia, S. Passerini, J. Power Sources 97 (2001) 790.
[43] G.B. Appetecchi, S. Passerini, J. Electrochem. Soc. 149 (2002) A891.
[44] H. Cheradame, P. Niddam-Mercier, Faraday Discuss. Chem. Soc. 88 (1989) 77.
[45] M.A. Ratner, D.F. Shriver, Mater. Res. Soc. Bull. (1989) 39.